Photochemical & Photobiological Sciences (2022) 21:2127–2138
https://doi.org/10.1007/s43630-022-00283-3

ORIGINAL PAPERS

Composite TiO_2 films modified by CeO_2 and SiO_2 for the photocatalytic removal of water pollutants

Jakub Rusek[1] · Michal Baudys[1] · Omri Toker[2] · Šárka Paušová[1] · Yaron Paz[2] · Josef Krýsa[1]

Received: 9 March 2022 / Accepted: 1 August 2022 / Published online: 18 August 2022

Abstract

TiO_2 particles of high photocatalytic activity immobilised on various substrates usually suffer from low mechanical stability. This can be overcome by the utilisation of an inorganic binder and/or incorporation in a robust hydrophobic matrix based on rare-earth metal oxides (REOs). Furthermore, intrinsic hydrophobicity of REOs may result in an increased affinity of TiO_2-REOs composites to non-polar aqueous pollutants. Therefore, in the present work, three methods were used for the fabrication of composite TiO_2/CeO_2 films for photocatalytic removal of dye Acid Orange 7 and the herbicide monuron, as representing polar and non-polar pollutants, respectively. In the first method, the composition of a paste containing photoactive TiO_2 particles and $CeCl_3$ or $Ce(NO_3)_3$ as CeO_2 precursors was optimised. This paste was deposited on glass by doctor blading. The second method consisted of the deposition of thin layers of CeO_2 by spray coating over a particulate TiO_2 photocatalyst layer (prepared by drop casting or electrophoresis). Both approaches lead to composite films of similar photoactivity that of the pure TiO_2 layer, nevertheless films made by the first approach revealed better mechanical stability. The third method comprised of modifying a particulate TiO_2 film by an overlayer based on colloidal SiO_2 and tetraethoxysilane serving as binders, TiO_2 particles and cerium oxide precursors at varying concentrations. It was found that such an overlayer significantly improved the mechanical properties of the resulting coating. The use of cerium acetylacetonate as a CeO_2 precursor showed only a small increase in photocatalytic activity. On the other hand, deposition of SiO_2/TiO_2 dispersions containing CeO_2 nanoparticles resulted in significant improvement in the rate of photocatalytic removal of the herbicide monuron.

Graphical abstract

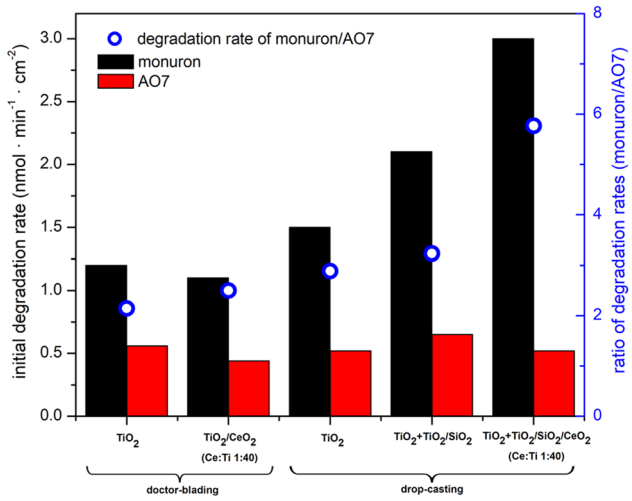

Keywords TiO_2 · CeO_2 · SiO_2 · Photocatalysis · Acid Orange 7 · Monuron · Water treatment

Extended author information available on the last page of the article

1 Introduction

Titanium dioxide (TiO_2), a non-toxic and inexpensive material, has been systematically utilised as a photocatalyst due to its chemical stability and high photocatalytic efficiency. Among various commercially available TiO_2 materials, the powder P25 (Evonik) [1] represents one of the most active photocatalysts thus serves as a benchmark, although there are other photocatalysts developed for more specific applications. Despite its superior properties, layers consisting of TiO_2 particles immobilised on various substrates usually suffer from low mechanical stability. This can be overcome by the utilisation of an inorganic binder, made from an appropriate oxide or hydroxide. Due to the intrinsic hydrophobicity of REOs [2–5], the resulting composite TiO_2-REOs layers may exhibit increased affinity to sparingly soluble non-polar aqueous pollutants. Thus, we aimed to develop efficient photocatalytic materials based on TiO_2 incorporated in a robust hydrophobic matrix based on rare-earth metal oxides (CeO_2, La_2O_3, Yb_2O_3) with expected high affinity to non-polar species resulting in the possible application in wastewater treatment. Among various REOs, cerium (IV) oxide (CeO_2) has been attracting our interest at first.

Rare-earth oxides are promising candidates for the fabrication of hydrophobic surfaces. Their robustness in applications under various harsh conditions has been demonstrated in several experimental studies [2, 3, 6, 7]. However, doubts remain as to the wettability of REOs. Reports demonstrating their intrinsic hydrophobicity [2–5] have been countered with claims that they are inherently hydrophilic [8, 9]. Their hydrophobic nature (resulting in water-contact angles exceeding 90°) can be attributed to their unique electronic structure [5] or to the adsorption of volatile organic compounds [8, 9]. Previous studies indicated that the deposition of thin CeO_2 films of desired wettability was a challenging task. Moreover, the wettability and other properties of thin ceramic CeO_2 films depends on the deposition technique and on associated process parameters.

Besides influencing surface hydrophobicity, CeO_2 has been also reported to improve photocatalytic properties when combined with TiO_2 [10, 11]. For example, a CeO_2/TiO_2 composite with CeO_2 content 1–10 mol % increased the photocatalytic conversion of toluene up to 3 times when compared to the bare TiO_2 [10]. Another study showed that the coating of TiO_2 nanoparticles by atomic layer deposition (ALD) of CeO_2 resulted in photoactivity enhancement over uncoated TiO_2 for the degradation of MB, that was attributed to formation of e^-/h^+ pair trap centres and reduction of e^-/h^+ recombination rate [11].

TiO_2 thin films consisting of TiO_2 particles can be conventionally prepared using a simple doctor blading where a paste of TiO_2 particles is blended with additives (e.g. thickeners, binders, surfactants, plasticisers), and such paste is coated on various substrates following by calcination. Another deposition technique is drop casting from aqueous TiO_2 particle suspensions [12] and electrophoretic deposition from a suspension of TiO_2 particles in methanol [13]. Such fabricated particulate films have high photocatalytic activity but on the other hand might suffer from low mechanical stability.

The present approach of fabrication of composite TiO_2/CeO_2 layers is thus based on the incorporation of CeO_2 precursors (chlorides, nitrates) to the TiO_2 paste to be then deposited by doctor blading. Another approach is the deposition of a CeO_2 precursor over a TiO_2 particulate layer; this method may result also in a significant improvement of mechanical properties. Such overlayer can be deposited by spray pyrolysis of metal salt solutions, a comparatively simple and versatile technique for the preparation of homogeneous thin films of CeO_2 [14–19]. Alternatively, a CeO_2 overlayer can be also deposited by a spray or dip coating of a solution of CeO_2 precursor or suspension of CeO_2 particles with optional subsequent calcination.

The aim of this work was the fabrication of mechanically stable photoactive composite TiO_2/CeO_2 layers by modifying particulate TiO_2 layers with various CeO_2 precursors, or, alternatively, by partial overcoating of such layers with cerium oxides. Photoactivity was evaluated using two model substances, the herbicide monuron as a representative of a non-polar pollutant and the anionic dye Acid Orange 7 (AO7) as a representative of a polar pollutant.

2 Experimental

2.1 Materials/chemicals

Microscope slides (Thermo Scientific, Menzel–Gläser, size 76×26 mm^2, 1 mm thick) were used as the supporting substrates. An aqueous suspension of TiO_2 particles (P25, Aeroxide, Evonik industries, Lot. No.: 616031498) was used for the preparation of TiO_2 layers. CeO_2 precursors ($CeCl_3$ (Sigma Aldrich, 99.9%), $Ce(NO_3)_3$ (Sigma Aldrich, 99%) and $Ce(AcAc)_3$ (Sigma Aldrich, 381403)) and two types of CeO_2 particles ("CeO_2 nano" (Sigma Aldrich, particle size 25 nm (BET), 544841 and CeO_2 (Sigma Aldrich, 99.0%, 22390-F)) were used for the preparation of CeO_2 layers.

The chemicals used were absolute ethanol (Penta, > 99.8%), TEOS (Tetraethoxysilan, Sigma Aldrich, 98%, R.G.), colloidal silica (Levasil CS30-125 MS, Vodní Sklo a.s.), HCl (Penta, 35%, A.G.), isopropyl alcohol (Lach-Ner, s.r.o., > 99.99%, G.R.), hydroxyethylcellulose (Fluka Analytical). Monuron (Sigma Aldrich, 99%, Lot.

No.: 06805EN) and Acid Orange 7 (Sigma Aldrich, Lot. No:10903HC-485) were used as model pollutants.

2.2 Films preparation

Three methods were used for the fabrication of composite TiO_2/CeO_2 films. Figure 1 shows an illustrative scheme of these different types of samples.

2.2.1 Doctor blading

A paste was prepared by mixing the following solutions/suspensions. Hydroxyethylcellulose (HEC) (0.5 g in 12.5 ml of distilled water (DW)) was mixed for 5 min. Then the following was added: (i) TiO_2 suspension (1 g in 5 ml of DW mixed for 20 min, following by sonication for 5 min.) or (ii) aqueous solutions of $CeCl_3$ at predefined concentrations or (iii) TiO_2 suspension (1 g in 5 ml of $CeCl_3$ or $Ce(NO_3)_3$ solution (at predefined concentrations) mixed for 20 min, then sonicated for 5 min). Pastes of different molar ratios of CeO_2 precursor/TiO_2 were deposited on the soda-lime glass by doctor blading. The deposited films were dried at 60 °C and then calcined at 500 °C for 1 h to remove the thickener (HEC) and transform the precursor to CeO_2. The thickness of the film was measured by profilometry. Layer thickness was at least 2 µm, which makes it an optically-thick film, in terms of light absorption as shown previously for the case of P25 layer where layer with thickness 2 µm (mass 0.2 mg/cm^2) absorbs more than 95% of incident light [20].

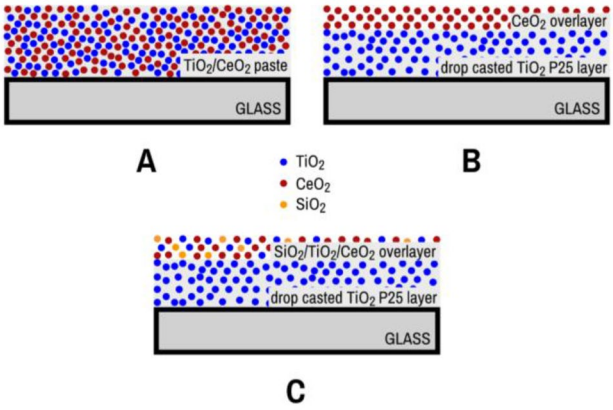

Fig. 1 An illustrative scheme of three types of composite TiO_2/CeO_2 layers. A paste containing TiO_2 and CeO_2 particles deposited by doctor blading and calcination at 500 °C (**A**), CeO_2 layer deposited over a particulate TiO_2 layer (**B**) and a composite $SiO_2/TiO_2/CeO_2$ layer deposited over a particulate TiO_2 layer (**C**)

2.2.2 Deposition of a CeO_2 overlayer over a particulate TiO_2 layer

Underlying TiO_2 P25 layers were prepared using drop casting of aqueous TiO_2 suspension (2.5 g · dm^{-3}) and electrophoretic deposition from methanolic TiO_2 suspension (10 g · dm^{-3}) at 10 V [13]. In the case of drop casting, coverage of TiO_2 was controlled by the volume of deposited suspension, in the case of electrophoretic deposition coverage of TiO_2 was controlled by the electrophoresis time.

CeO_2 overlayers were prepared by spray pyrolysis of an aqueous solution of cerium chloride ($c = 0.05$ mol · dm^{-3}) using a homemade automatic spraying system (air pressure 4 bar, deposition temperature 450 °C). The thickness of the CeO_2 layer was 500 nm as measured by profilometry. CeO_2 overlayers were also prepared utilising spray and dip coating of cerium acetylacetonate (0.01 mol · dm^{-3}) in ethanol with subsequent calcination at 500 °C for 1 h. Here, thickness of the CeO_2 layer was 100 and 200 nm, respectively.

2.2.3 Deposition of a $SiO_2/TiO_2/CeO_2$ overlayer over a particulate TiO_2 layer

Underlying TiO_2 P25 layers were prepared using drop casting of TiO_2 suspension (2.5 g · dm^{-3}), the coverage amount being 0.5 mg · cm^{-2}. Such prepared underlayers were modified by overlayers comprising of SiO_2/TiO_2 and cerium acetylacetonate or CeO_2 nanoparticles. 3.2 ml of TiO_2 P25 aqueous suspension ($c = 240$ g · dm^{-3}) was added under vigorous stirring to the SiO_2 binder consisting of 1.4 ml tetraethoxysilane (TEOS), 2.2 ml colloidal SiO_2 (Ludox) and 6.4 ml isopropanol. The mixture was diluted with n-propanol (1:1.35). Nanoparticles of CeO_2 were mixed under vigorous stirring in the suspension of TiO_2 to get a molar ratio Ce:Ti = 1:40, 1:20 and 1:10. Such suspensions were deposited on the glass substrate by (i) spray coating (airbrush) and by (ii) dip coating (dipping and withdrawal speed was 30 mm min^{-1} with a 60 s delay) and subsequent annealing at 500 °C for 1 h.

2.3 Film characterisation

The prepared composite films were characterised by XRD, SEM and contact angle measurement. The mechanical stability (adhesion to the substrate) was demonstrated using the Scotch Tape Test (Scotch Magic™ Tape, width 19 mm), UV–VIS spectroscopy and via long term exposure in an aqueous environment.

The photocatalytic activity of the composite films was evaluated using two model substances, the herbicide monuron as a representative of a non-polar pollutant and the anionic dye Acid Orange 7 (AO7) as a representative of a polar pollutant. A magnetically-stirred water-cooled rectangular glass reactor was used [21]. Samples with catalyst layers

were irradiated by Sylvania Lynx CFS 11 W BL350 fluorescent UV light tubes. These tubes emit irradiation in the wavelength range from 320 to 390 nm with a maximum at 355 nm. The light intensity was 1.9 mW · cm^{-2}.The initial concentration of AO7 and monuron was $1 \cdot 10^{-4}$ mol dm^{-3}. The initial pH of both model pollutants was 5.7. The irradiated area and the reactor volume were (2.5 × 4) cm^2 and 25 ml, respectively. The concentration of AO7 was measured using UV–VIS spectroscopy [21], the concentration of monuron was followed by HPLC analysis [22], employing a Shimadzu modular system Nexera lite with photo diode array detector SPD-M40. A mobile phase methanol/water (60:40, v/v) was applied, with a flow rate of 1 ml min^{-1} and a LiChrospher 100 RP-18 column (type LiChroCART 125–4, Merck, Germany). The concentration of each pollutant was followed as a function of irradiation time. From the concentration decay the initial degradation rate was calculated as described elsewhere [21].

3 Results

3.1 TiO_2/CeO_2 films prepared by doctor blading

Table 1 summarizes the surface mass and water-contact angles of composite films of various molar ratios of Ce:Ti. Surprisingly, pure CeO_2 layer exhibited a low contact angle of about 25°. In the case of a Ce:Ti ratio 1:1 and 1:2, the contact angle was higher (in the range of 30–60°). When nitrate was used as a precursor, the contact angle was even lower (about 20°). We studied in detail the influence of post-calcination at 500 °C for 1 h in air and following exposure to the air (see Figure S1 in SI). It was observed that immediately after calcination, the contact angle became lower than 5°, nevertheless, within 50 min it increased to almost 50°, which is much higher that the contact angle of as prepared CeO_2 layer. These findings support previous claims that the hydrophobicity of REOs is primarily determined by the environment to which the REO surface is exposed [7].

Table 1 Parameters of TiO_2/CeO_2 thin films prepared from pastes by doctor blading

Ratio Ce:Ti	Precursor	Mass of deposit (mg · cm^{-2})	Contact angle (°)
Pure CeO_2	$CeCl_3$	0.17	25
Pure TiO_2	–	0.23	–
1:1	$CeCl_3$	0.37	43
1:1	$Ce(NO_3)_3$	0.58	21
1:1.3	$CeCl_3$	0.48	29
1:2	$CeCl_3$	0.27	62

Thus, the measured values in Table 1 cannot be regarded as reflecting the true property of the material.

The TiO_2/CeO_2 films having Ce:Ti ratios of 1:2 and 1:1 showed very good mechanical stability (see Figure S6 in SI). SEM morphology and XRD difractogram of films with Ce:Ti ratio of 1:2 are shown in Figure S2 and Figure S3, respectively. The film contained crystalline CeO_2 having a fluorite-type cubic structure, together with anatase and rutile lines corresponding to P25 TiO_2 particles. The photocatalytic activity of the prepared films was evaluated based on the degradation of the anionic dye Acid Orange 7 (AO7) in an aqueous solution under UV light irradiation. The time dependence of AO7 concentration during irradiation is shown in Figure S4 (in SI). Films modified with CeO_2 exhibited a significant decrease in photocatalytic activity (app. 5 times) compared with films containing only TiO_2. This decrease cannot be explained by the lower content of TiO_2 in the CeO_2 modified film (66% vs. 100% in unmodified film). Anyway, it seems that the amount of CeO_2 has to be decreased.

In the next step instead of CeO_2 precursors CeO_2 particles (BET surface area 47 m^2/g) were added to the paste and the Ce:Ti ratio was decreased to 1:10, 1:20 and 1:40.

Table 2 summarises the surface mass of TiO_2/CeO_2 films of various molar ratios of Ce:Ti. Profilometry of compositeTiO_2 layer (see Figure S5 in SI) shows rather smooth character of the layer and thickness around 6–7 µm.

The photocatalytic activity was evaluated using Acid Orange 7 (AO7) as a representative of a polar pollutant and the herbicide monuron as a representative of a non-polar pollutant. Figure 2a and Fig. 2b show the time dependence of AO7 and monuron concentration during irradiation, respectively. Adsorption of monuron on the composite TiO_2-CeO_2 paste layers (Fig. 2b, open rectangles) was negligible, on the other side adsorption of AO7 (Fig. 2a, open rectangles) was not negligible (decrease of concentration was about 2% after 30 min and then almost constant up to 4 h). Therefore, the measured concentrations of AO7 were corrected for adsorption in the dark and resulting AO7 concentrations are shown as a function of irradiation in Fig. 2a. The photocatalytic activity can be compared via apparent first order rate constant (k, min^{-1}). Another approach for the comparison

Table 2 Parameters of TiO_2/CeO_2 thin films prepared from pastes with nanoparticles of CeO_2 by doctor blading

Sample	Ratio Ce:Ti	Mass of deposit (mg · cm^{-2})
N4	Pure TiO_2	0.9
N7	1:40	1.0
N13	1:20	1.3
N15	1:10	1.3

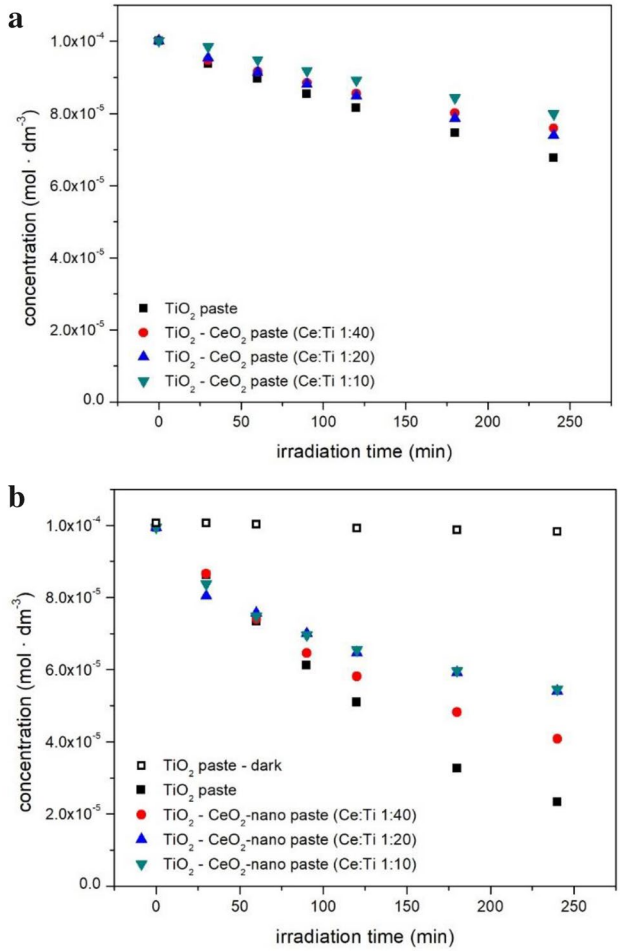

Fig. 2 **a** Photocatalytic degradation of AO7 on composite TiO_2/CeO_2 films of various Ce:Ti ratio prepared by doctor blading. Photocatalyst mass 0.9 – 1.3 mg · cm^{-2} (see Table 2). **b** Photocatalytic degradation of monuron on composite TiO_2/CeO_2 films of various Ce:Ti ratio prepared by doctor blading. Photocatalyst mass 0.9 – 1.3 mg · cm^{-2} (see Table 2)

of photocatalytic activity is via initial degradation rate (r_i, nmol · cm^{-2} · min^{-1}), calculated based on the concentration decay during first 60 min.

The initial degradation rates of monuron and Acid Orange 7 with composite TiO_2/CeO_2 layers of various Ce:Ti ratios, prepared by doctor blading are shown in Fig. 3. Error bars (calculated from three identical experiments) were included to evaluate the significance of observed differences. For AO7 there is a decrease about 40% for Ce:Ti ratio 1:40 and about 10–20% for Ce:Ti ratio of 1:20 and 1:10. For monuron there is a decrease about 15% for Ce:Ti ratio 1:40, but the difference between various Ce:Ti ratios is within an experimental error.

This decrease is not as strong as in the case of pastes with much higher Ce:Ti as shown in Figure S4 (in SI). Figure 3 also shows the ratio of initial degradation rates of both

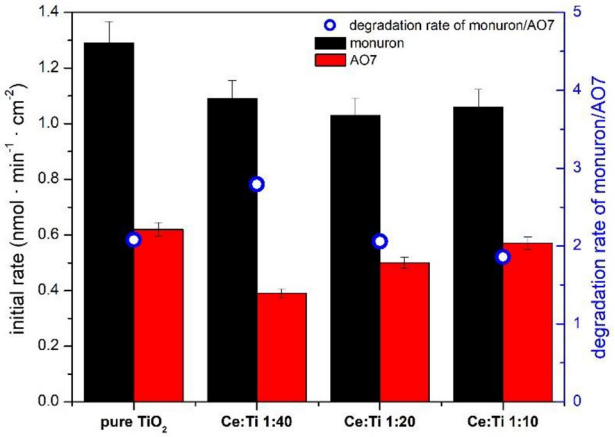

Fig. 3 Initial degradation rate of monuron and Acid Orange 7 (left axis) and the ratio of initial degradation rates of both pollutants (right axis) for composite TiO_2/CeO_2 layers of various Ce:Ti ratio prepared by doctor blading with CeO_2 nano. The irradiated area was 10 cm^2. Photocatalyst mass 0.9 – 1.3 mg · cm^{-2} (see Table 2)

pollutants, it can be seen that this parameter is around 2 and does not depend on the Ce:Ti ratio. All in all, for this type of films, the addition of cerium oxide did not improve the photocatalytic activity for both AO7 and monuron.

3.2 TiO_2/CeO_2 films - CeO_2 overlayers on particulate TiO_2 layers

Composite layers consisting of TiO_2 particles and CeO_2 particles, prepared by doctor blading (3.1) were mechanically stable but exhibited lower photocatalytic activity than pure TiO_2 layers. The next approach for the preparation of composite film consisted of two steps. The first step was the deposition of particulate TiO_2 layer of known mass and thickness, the second step was the coverage of particulate TiO_2 layer by an CeO_2 overlayer.

Particulate TiO_2 layers were prepared by drop casting and electrophoretic deposition from suspension of TiO_2 particles (P25). To observe the adhesion and cohesion of particles, a fixed area of samples (5 cm^2) was covered with a scotch tape, then a weight was put for a fixed time on the tape and then the tape was removed. In general, the adhesion of TiO_2 layers to the substrate decreased with the increasing deposited amount of TiO_2. It was found previously that the deposited mass of TiO_2 higher than 0.5 mg · cm^{-2} does not improve photocatalytic activity [20]. Therefore, layer of such mass was investigated in detail. The results of the Scotch tape test (the surface images of TiO_2 layer and corresponding tape after the scotch tape test) are shown for both nanoparticulate layers of the same deposit mass (0.5 mg · cm^{-2}) and thickness (4.5 µm) in Figure S7 (in SI). In both cases there were particles that remained on the scotch tape after its removal from the layer. But the images of the films after the Scotch

tape test show that the nanoparticulate TiO_2 layers prepared by drop casting of TiO_2 particles had much better adhesion to the substrate in comparison with TiO_2 layer prepared by electrophoretic deposition.

At first, particulate TiO_2 films (0.5 mg · cm^{-2}) were covered by an optimised CeO_2 coating (thickness 500 nm) utilising spray pyrolysis of $CeCl_3$. The observed photocatalytic activity of composite films with CeO_2 coating fabricated by spray pyrolysis (shown in Figure S8 in SI) was significantly lower (5 times) than the original particulate TiO_2 layer prepared by drop casting. Very poor photocatalytic activity can be explained by the fact that particulate TiO_2 films were overcoated by CeO_2 films and thus shielded TiO_2 from incident light. As CeO_2 is also a semiconductor and may contribute to the overall activity of a composite layer, photocatalytic activity of pristine CeO_2 layer was also evaluated and found negligible (see Figure S8 in SI).

As a next step, particulate TiO_2 films (0.5 mg · cm^{-2}) were covered by a thinner coating (100 and 200 nm) of CeO_2 using cerium acetylacetonate as a precursor to make the TiO_2 particles less shielded and more accessible to the aqueous media. Spray and dip coating were used for the deposition of this overlayer. Photocatalytic degradation of the herbicide monuron in aqueous solution on such fabricated composite films is shown in Fig. 4. Although the thickness of the CeO_2 overlayer was only 100 nm, the resulting composite layer had significantly lower photoactivity than the original particulate TiO_2 layer. With increasing thickness of CeO_2 overlayer to 200 nm we observed even stronger decrease in photocatalytic activity of the composite layer (method of overlayer deposition (spray or dip coating) does not play any role). Explanation for very poor photocatalytic activity is similar to the case of composite films with an overlayer prepared by spray pyrolysis. Particulate TiO_2 films were overcoated by CeO_2 films and thus shielded TiO_2 from incident light. It should be noted that previous studies showed that a few (less than 12) atomic layers of silica [23] or alumina [24] are sufficient to prevent any photocatalytic activity. Hence, it is quite interesting that some activity is still found with an overcoated layer of 100 nm. This activity may indicate that the overcoating layer is porous and does not fully cover the underlying titania.

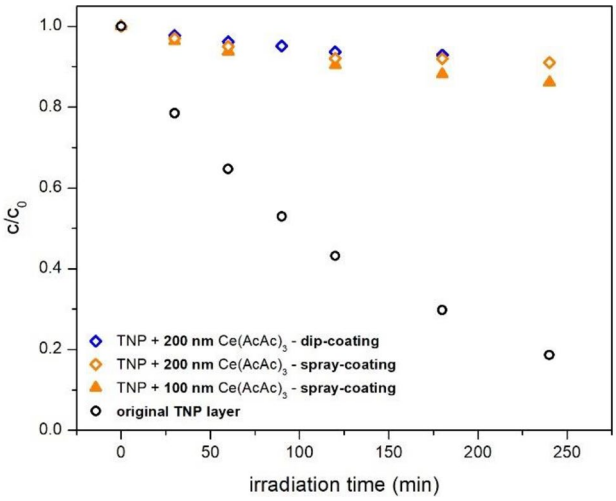

Fig. 4 The kinetics of photocatalytic degradation of monuron, by particulate TiO_2 layers (TNP),overcoated with a CeO_2 overlayer of different thickness., Here, the thickness of the TNP was 4.5 µm, and the ceria precursor was 0,01 mol · dm^{-3} $Ce(AcAc)_3$) in ethanol. The deposition was performed by dip coating or spray coating, following by calcination at 500 °C. Photocatalyst mass 0.5 mg · cm^{-2}

3.3 $SiO_2/TiO_2/CeO_2$ films - $SiO_2/TiO_2/CeO_2$ overlayers on a particulate TiO_2 layers

The third approach to the preparation of ceria-containing photocatalysts was based on the improvement of the cerium oxide-based overlayer and consisted of two steps: (i) deposition of particulate TiO_2 underlayer by drop casting, (ii) deposition of an overlayer consisting of TiO_2 particles, a binder based on a mixture of colloidal SiO_2 and tetraethoxysilane (TEOS) and cerium acetylacetonate as cerium oxide precursor or CeO_2 nanoparticles in various proportions. The ratio of Si:Ti in all overlayers was 2:1 as determined by EDX analysis.

3.3.1 Particulate TiO_2 layers (drop casting) modified by an overlayer consisting of TiO_2 particles and cerium acetylacetonate in SiO_2 binder

A particulate TiO_2 layer of known mass (0.5 mg · cm^{-2}) was deposited by drop casting from an aqueous suspension. Then, an overlayer containing cerium oxide precursor was deposited by spray coating (cerium acetylacetonate in ethanol mixed with TiO_2 particles and SiO_2 binder (ratio Ce:Ti = 1:40)) at room temperature, following by annealing at 500 °C. The thickness of such overlayers was 200 nm as measured by profilometry.

The kinetics of the photocatalytic oxidation of monuron are shown in Fig. 5. A thin layer comprising of nothing but the overlayer deposited on glass showed very small photocatalytic activity (see Fig. 5, black triangles). But when such an overlayer was deposited on the TiO_2 layer (prepared by drop casting) (see Fig. 5, open spheres), the photocatalytic activity was found to be better than the original layer (Fig. 5, black diamonds). Another advantage was a significant increase in the mechanical stability of the coating (see Fig. 9).

The improvement in photoactivity could be due to the presence of CeO_2 as well as due to the presence of the SiO_2 binder. To clarify this, particulate TiO_2 layers were also covered by an overlayer consisting of TiO_2 particles,

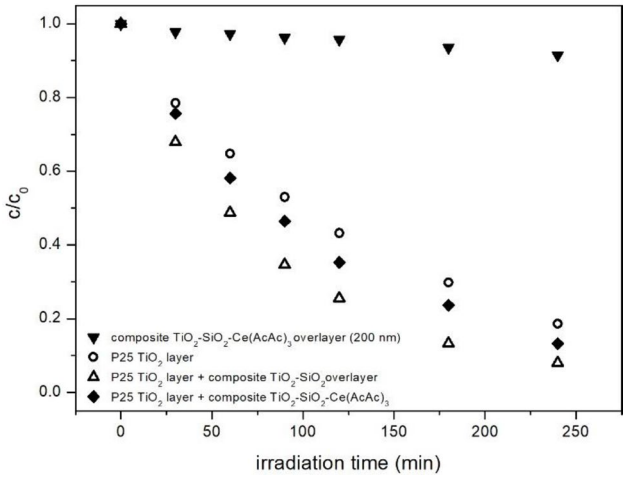

Fig. 5 The concentration of monuron as a function of UV irradiation time on TiO_2 photocatalyst coatings modified by an overlayer containing cerium oxide. ○ P25 TiO_2 layer (drop casting), ▼ spray-coated overlayer prepared from TiO_2 particles, SiO_2 binder and $Ce(AcAc)_3$ (200 nm), ◆ P25 TiO_2 layer + spray-coated overlayer containing TiO_2 particles, SiO_2 binder and cerium oxide prepared from $Ce(AcAc)_3$, Δ P25 TiO_2 layer + spray-coated overlayer containing TiO_2 particles and SiO_2 binder. Photocatalyst mass 0.5 mg · cm^{-2}

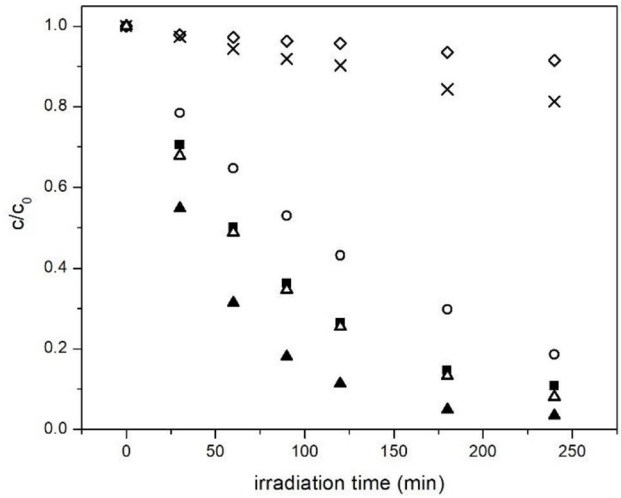

Fig. 6 Concentration of monuron as a function of UV irradiation time of TiO_2 photocatalyst coatings modified by overlayer $SiO_2/TiO_2/CeO_2$ consisting of CeO_2 and TiO_2 nanoparticles and SiO_2 binder. ○ P25 TiO_2 layer (drop casting), ◇ spray-coated $SiO_2/TiO_2/CeO_2$ layer (200 nm), x dip-coated $SiO_2/TiO_2/CeO_2$ layer (250 nm), Δ P25 TiO_2 layer + spray-coated overlayer containing TiO_2 particles and SiO_2 binder (250 nm), ■ P25 TiO_2 layer + spray-coated $SiO_2/TiO_2/CeO_2$ overlayer (200 nm), ▲ P25 TiO_2 layer + dip-coated $SiO_2/TiO_2/CeO_2$ overlayer (250 nm). Photocatalyst mass 0.5 mg · cm^{-2}

SiO_2 binder but without CeO_2 precursor. The results clearly showed that the main factor here was the presence of the silica binder such that the addition of $Ce(AcAc)_3$ as CeO_2 precursor had hardly any positive effect.

3.3.2 Particulate TiO_2 layers (drop casting) modified by an overlayer consisting of TiO_2 and CeO_2 particles in SiO_2 binder

In the next phase, attention was focussed on the integrating CeO_2 nanoparticles (instead of CeO_2 precursors) with TiO_2 particles and SiO_2 binder. The resulting $TiO_2/SiO_2/CeO_2$ suspension was deposited on the glass substrate using spray coating (thickness 200 nm) and dip coating (thickness 250 nm). These two overlayers (200 and 250 nm) were also used for the coverage of TiO_2 particulate layers prepared by drop casting (0.5 mg · cm^{-2}). The kinetics of photocatalytic oxidation of monuron on such coatings are shown in Fig. 6.

$TiO_2/SiO_2/CeO_2$ layers prepared by dip and spray coating on glass exhibit photocatalytic activity (even very small) for monuron degradation, but a more interesting effect was obtained after the deposition of such $TiO_2/SiO_2/CeO_2$ overlayers on the TiO_2 P25 particulate layer. Both composite layers showed significant improvement in photocatalytic degradation of monuron compared to the particulate TiO_2 P25 layer. However, in the case of spray coating, the composite film exhibited a similar performance as the TiO_2 P25 layer covered by TiO_2-SiO_2 overlayer without CeO_2. No further improvement was indicated with CeO_2 addition. But on the other hand, the overlayer deposited by dip coating exhibited much better performance even in comparison with TiO_2 P25 layer covered by TiO_2-SiO_2 overlayer. The possible explanation could be in better penetration of the dip-coated overlayer into the porous TiO_2 underlayer. However, the thickness of both overlayer coatings (measured on glass substrate by profilometry) was similar (200 and 250 nm).

In the next step $TiO_2/SiO_2/CeO_2$ overlayers of various Ce:Ti ratios were deposited by dip coating on the TiO_2 P25 particulate layer and used for photocatalytic degradation of monuron and Acid Orange 7. The kinetics of photocatalytic oxidation of monuron on such coatings are shown in Fig. 7. The corresponding first order constants and initial degradation rates are shown in Table S1 (in SI). The comparison of initial degradation rates of both model pollutants on various coatings, namely particulate TiO_2 layer, TiO_2 layer + SiO_2/TiO_2 overlayer and TiO_2 layer + $SiO_2/TiO_2/CeO_2$ overalyers containing CeO_2 nano and CeO_2 particles of different Ce:Ti molar ratio is shown in Fig. 8. Coverage of the TiO_2 P25 layer by TiO_2-SiO_2 overlayer without CeO_2 results in the similar increase of initial degradation rates for both AO7 and monuron. But the presence of CeO_2 particles in TiO_2-SiO_2 overlayer exhibits improvement only in the case of monuron which means that the ratio of initial degradation rates of both pollutants significantly increased. The positive effect of the incorporation of CeO_2 particles in TiO_2-SiO_2 overlayer can be explained by increasing the adsorption of hydrophobic compound or by inducing charge separation. It was proved

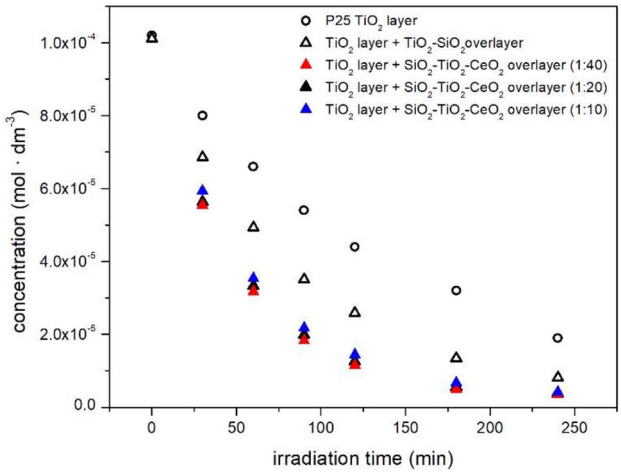

Fig. 7 Concentration of monuron as a function of UV irradiation time of TiO_2 photocatalyst coatings modified by overlayer $SiO_2/TiO_2/CeO_2$ consisting of CeO_2 and TiO_2 nanoparticles and SiO_2 binder. ○ P25 TiO_2 layer (drop casting), Δ P25 TiO_2 layer + SiO_2/TiO_2 overlayer, ▲ P25 TiO_2 layer + $SiO_2/TiO_2/CeO_2$ overlayer (Ce:Ti = 1:40), ▲ P25 TiO_2 layer + $SiO_2/TiO_2/CeO_2$ overlayer (Ce:Ti = 1:20), ▲ P25 TiO_2 layer + $SiO_2/TiO_2/CeO_2$ overlayer (Ce:Ti = 1:10). Photocatalyst mass 0.5 mg · cm^{-2}

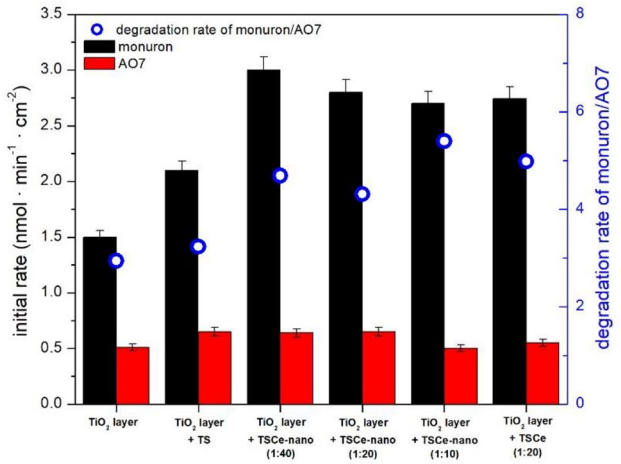

Fig.8 Initial degradation rate of monuron and Acid Orange 7 (left axis) and the ratio of initial degradation rates of both polutants (right axis) for the drop-casted TiO_2 particulate layer and that covered by various (dip coated) composite overlayers containing CeO_2 nano or CeO_2 particles in different Ce:Ti molar ratio in SiO_2 binder. The irradiated area was 10 cm^2. Photocatalyst mass 0.5 mg · cm^{-2}. (TS means TiO_2/SiO_2, TSCe-nano means $TiO_2/SiO_2/CeO_2$ nano and TSCe means $TiO_2/SiO_2/CeO_2$)

in our recent work that particles of rare-earth oxides (oxides of Er, La, Gd and Ce) incorporated in TiO_2-SiO_2 coatings assist in photocatalytic degradation of hydrophobic pollutant ciprofloxacin by serving as electron sinks [25]. The later explanation thus seems to be more probable.

The beneficial effect of silica on the degradation kinetics of the non-polar pollutant monuron could be explained via the "Adsorb & Shuttle" phenomenon in which molecules are being adsorbed in the vicinity of photocatalytic domains and then diffuse to the photocatalytic domains [26]. This phenomenon would assists in adsorbing monuron in close proximity to the photocatalyst. It can be supported by our recent work where we studied the effect of modifying TiO_2 with REOs of the lanthanide family (Er, La, Gd, Ce) on the photocatalytic activity towards degrading ciprofloxacin, another model non-polar compound, and show that the hydrophobicity of the silica binder plays an important role in promoting ciprofloxacin degradation [25]. The fact that the presence of silica had a positive effect also on the degradation kinetics of Acid Orange 7 suggests that other mechanisms could be involved. In that context, it is noteworthy that a composite of silica-titania was found to be very efficient in the photocatalytic degradation of the water-soluble dye rhodamine 6G, which tends to adsorb on silica but not on titanium dioxide [27], so apparently the effect of silicon dioxide is not limited to hydrophobic compounds. In addition, we cannot negate the possibility that the effect of silica was due to increasing the surface area of the films. This explanation is in line with the smaller diameter of the silicon dioxide particles.

For Ce:Ti ratio 1:20, the influence of two types of CeO_2 was investigated. XRD patterns are shown in Figure S9 (in SI), crystal size (calculated form XRD) and BET surface area are given in Table S2 (in SI). Calculated crystal size is similar, 20 nm for "**CeO_2** nano" particles and 31 nm for **CeO_2** particles, while BET surface area is for CeO_2 particles 8 $m^2 \cdot g^{-1}$, for "CeO_2 nano" particles it is 6 times higher (47 $m^2 \cdot g^{-1}$). In the case where CeO_2–nano particles were replaced by CeO_2 particles, degradation rates of both pollutants are similar. This suggests that neither the particle size of CeO_2 nor its surface area plays a significant role.

The stability of the $TiO_2/SiO_2/CeO_2$ composite layers in photocatalytic applications was verified by repeated photocatalytic degradations of monuron. 5 cycles of repeated use were performed and then the effect of regeneration under UV light irradiation was tested (see Figure S10 in SI). The mechanical stability of composite layers was sufficient (no particle loss was detected during repeated photocatalytic degradation). After 5 cycles of repeated photocatalytic degradation, XRD analysis did not show any change in the phase composition, also SEM morphology of the composite layers did not change (see Figs. S11 and S12 in SI).

3.3.3 Film morphology and mechanical stability

To determine the mechanical stability of the composite TiO_2 film, a scotch tape test was performed on the TiO_2 particulate layer covered by dip-coated SiO_2/TiO_2 overlayer containing CeO_2 nanoparticles (see Fig. 9b). As shown in Fig. 9,

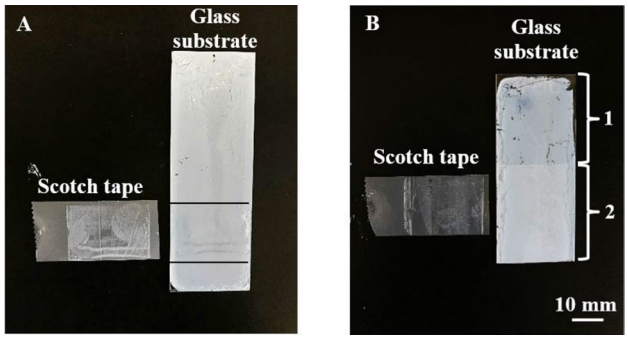

Fig. 9 Scotch tape test. The comparison of mechanical stability of the TiO_2 layer (coverage 0.5 mg · cm^{-2}) (**A**) and composite layer – TiO_2 layer partly covered by the TiO_2-SiO_2-CeO_2 overlayer (**B**), molar ratio of Ce:Ti = 1:20. Numbers in the picture B means: 1 – unmodified part of the layer and 2 – modified part of the layer, i.e. TiO_2 layer covered by the TiO_2-SiO_2-CeO_2 overlayer

the amount of material transferred to the scotch tape was larger in the case of the particulate layer (Fig. 9a) than that of the composite TiO_2 layer (Fig. 9b). This means that there was a significant increase in the mechanical stability of the TiO_2 layer following modification with the TiO_2-SiO_2-CeO_2 overlayer.

To quantify the difference in the mechanical stability of the TiO_2 layers the transmittance of the films was measured in the range of 300–800 nm, prior to and after performing the scotch tape test. The UV–VIS spectra of the underlying TiO_2 particulate layers prepared by drop casting and that of the composite TiO_2 particulate layers covered byTiO_2-SiO_2-CeO_2 overlayer of molar ratio 1:20 (Ce:Ti) were corrected for the transmittance of the glass substrate and are shown in Figure S13 (in SI). In the case of the underlying drop-casted TiO_2 nanoparticulate layer, there were considerable differences in transmittance, before and after the scotch tape test (Figure S13a). On the other side, in the case of the composite layer (drop casted underlying TiO_2 nanoparticulate layer + TiO_2-SiO_2-CeO_2 overlayer), the values of transmittance were almost the same, before and after the scotch tape test (Figure S13b). The modification with an TiO_2-SiO_2-CeO_2 overlayer thus resulted in better adhesion to the substrate and therefore in higher mechanical stability.

The morphology of a drop-casted TiO_2 particulate layer and the morphology of the composite TiO_2/CeO_2 layer consisting of a drop-casted particulate TiO_2 layer with a dip-coated SiO_2/TiO_2/CeO_2 overlayer is shown in Fig. 10 and Fig. 11, respectively.

In the case of the particulate TiO_2 layer (Fig. 10), one can clearly see a typically open structure consisting of small particles of TiO_2 (size around 50 nm). In the case of films containing a SiO_2/TiO_2/CeO_2 overlayer (Fig. 11), one sees only a slight difference in morphology. The size of the TiO_2 particles in both films is around 50 nm, but due to the presence of a binder, agglomerates/clusters of particles are observed. This explains the better adhesion to the substrate. Film with different Ce:Ti ratio (1:20 and 1:40) did not show any significant difference in their surface morphology (see Figure S14 in SI).

Particle size around 50 nm is in agreement with the calculated crystalline size of TiO_2 (Scherrer equation) determined as 40 ± 20 nm. CeO_2 particles present in the overlayer had crystalline size 20 ± 5 nm, but due to the small Ce content (C:/Te ratio = 1:20) and similar size as TiO_2, both oxides could not be distinguished on the SEM images. The surface chemical composition of a composite TiO_2/CeO_2 layer (TiO_2 particulate layer modified by SiO_2/TiO_2/CeO_2 overlayer) done by EDX is shown in Table 3. The calculated Ti:Ce ratios were 43, 21 and 11, respectively, which are very close to the Ti:Ce ratios in the suspensions deposited by spray or dip coating. This

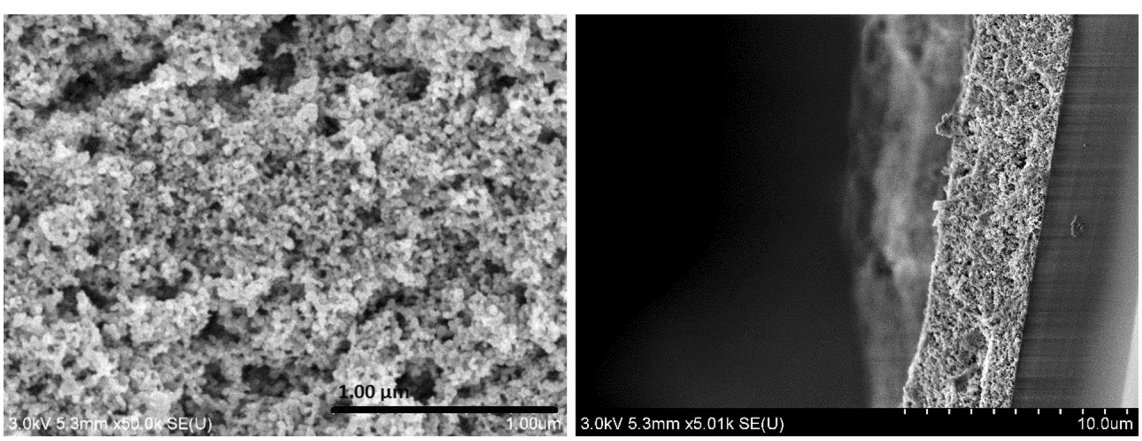

a **b**

Fig. 10 SEM micrographs of particulate TiO_2 P25 layer. **a** top view (0°), **b** cross-section (inclination 90°). Photocatalyst mass 0.5 mg · cm^{-2}

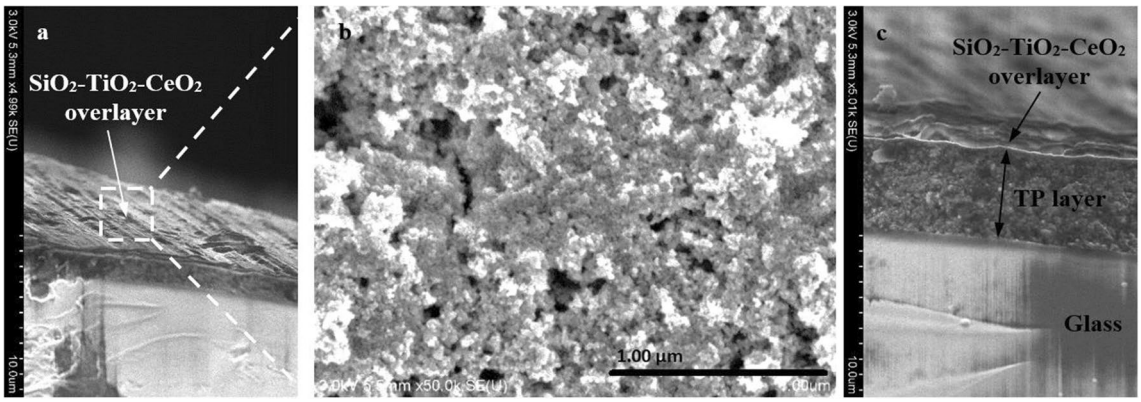

Fig. 11 SEM micrographs of a composite TiO_2/CeO_2 layer (TiO_2 particulate layer modified by $SiO_2/TiO_2/CeO_2$ nano overlayer, molar ratio Ce:Ti = 1:20) **a** cross-section (inclination 45°), **b** top view (0°), c) cross-section (inclination 90°). Photocatalyst mass 0.5 mg · cm^{-2}

confirms that the $SiO_2/TiO_2/CeO_2$ suspension was deposited homogeneously.

From cross-section SEM micrographs it follows that the thickness of the drop-casted TiO_2 layer was around 4.5 µm, and the thickness of the composite $SiO_2/TiO_2/CeO_2$ overlayer was around 300 nm. Profilometry was used as another method for the determination of layer thickness. The profile of drop-casted TiO_2 particulate layer (mass of deposit 0.5 mg · cm^{-2}) is shown in Figure S15a (in SI). The profile of a $SiO_2/TiO_2/CeO_2$ overlayer is shown in Figure S15b. The surface roughness is higher than in the case of layers prepared by doctor blading (see Figure S5 in SI), the measured thickness was lower, 4.5 ± 0.5 µm. Comparison of layer thicknesses (TiO_2 particulate layer and $SiO_2/TiO_2/CeO_2$ overlayer) obtained from SEM and profilometry is shown in Table S3 (in SI). Thicknesses of both layers obtained from SEM analysis and profilometry are in very good agreement.

The film prepared by drop casting with dip or spray-coated overlayer has higher roughness and thus higher surface area than the layer prepared by doctor blading. The difference between photocatalytic performance could be thus primary related to the film architecture which comes from a deposition method.

Table 3 Chemical composition of the composite TiO_2/CeO_2 layer (particulate TiO_2 layer modified by $SiO_2/TiO_2/CeO_2$ nano overlayer with different Ce:Ti molar ratio) and calculated Ti:Ce ratio

Sample	Element content (atomic %)				
	O	Si	Ti	Ce	Ti/Ce
TiO_2 layer + TSCe-nano (1:40)	66.2	21.0	9.7	0.23	43
TiO_2 layer + TSCe-nano (1:20)	70.0	17.5	10.7	0.50	21
TiO_2 layer + TSCe-nano (1:10)	68.8	18.1	10.5	0.95	11

4 Conclusion

Thin composite films of TiO_2 particles embedded in a CeO_2 matrix were produced using three methods. In the first approach, paste deposition by doctor blading, it was necessary to optimise the composition of the paste containing photoactive TiO_2 and $CeCl_3$, $Ce(NO_3)_3$ as precursors of CeO_2 or CeO_2 particles as well as the process conditions for the preparation of the composite layer. The resulting composite films were mechanically stable; however, the photoactivity was similar to that of pristine TiO_2.

In the second approach, thin layers of CeO_2 by spray or dip coating were deposited on particulate TiO_2 layers (prepared by drop casting and electrophoresis). The mechanical stability of such fabricated composite films in terms of adhesion to the substrate as well as stability in an aqueous environment was found to be satisfactory. But the photoactivity was lower than that of original pure TiO_2 films.

In the third approach, a TiO_2 layer prepared by drop casting was modified by an overlayer of various molar ratio Ti:Ce (40:1, 20:1 and 10:1) consisting of a binder (colloidal SiO_2 and TEOS as a film-forming substance), TiO_2 particles and various cerium oxide precursors. The dispersion of TiO_2 particles (P25) in the binder system deposited by spray or dip coating on the pre-prepared TiO_2 particle layers significantly improved the mechanical properties of the coating. The addition of acetylacetonate to the prepared binder system and its deposition resulted in only small increase in photocatalytic activity. Modification with an overlayer containing a SiO_2 binder without CeO_2 nanoparticles resulted in significant improvement in the mechanical properties as well as in a 30% increase (in comparison with the original pure TiO_2 layer) of initial degradation rates for both AO7 and monuron. Modification with an overlayer containing CeO_2 nanoparticles in a SiO_2 binder resulted in another 50% increase (in comparison with the TiO_2 layer covered

by a TiO_2/SiO_2 overlayer) but only in the case of the herbicide monuron, used as a model compound of a non-polar pollutant.

Supplementary Information The online version contains supplementary material available at https://doi.org/10.1007/s43630-022-00283-3.

Acknowledgements This work was supported by the Ministry of Education, Youth and Sport of the Czech Republic (project LTAIZ19011) and by the Israeli Ministry of Science (grant No. 3-16075).

Funding Ministerstvo Školství, Mládeže a Tělovýchovy, LTAIZ19011, Josef Krysa, Israeli Ministry of Science, No. 3-16075, Yaron Paz

Declarations

Conflicts of interest There are no conflicts to declare.

References

1. Ohtani, B., Prieto-Mahaney, O. O., Li, D., & Abe, R. (2010). What is Degussa (Evonik) P25? Crystalline composition analysis, reconstruction from isolated pure particles and photocatalytic activity test. *Journal of Photochemistry and Photobiology A: Chemistry, 216*, 179–182.
2. Azimi, G., Kwon, H.-M., & Varanasi, K. K. (2014). Superhydrophobic surfaces by laser ablation of rare-earth oxide ceramics. *MRS Communications, 4*, 95–99.
3. Bai, M., Kazi, H., Zhang, X., Liu, J., & Hussain, T. (2018). Robust hydrophobic surfaces from suspension HVOF thermal sprayed rare-earth oxide ceramics coatings. *Science and Reports, 8*, 1–8.
4. Fronzi, M., Assadi, M. H. N., & Hanaor, D. A. (2019). Theoretical insights into the hydrophobicity of low index CeO2 surfaces. *Applied Surface Science, 478*, 68–74.
5. Azimi, G., Dhiman, R., Kwon, H.-M., Paxson, A. T., & Varanasi, K. K. (2013). Hydrophobicity of rare-earth oxide ceramics. *Nature materials, 12*, 315–320.
6. Liang, J., Hu, Y., Fan, Y., & Chen, H. (2013). Formation of superhydrophobic cerium oxide surfaces on aluminum substrate and its corrosion resistance properties. *Surface and interface analysis, 45*, 1211–1216.
7. P. Singh, K. Srivatsa, On the wettability and optical properties of nanocrystalline CeO 2 thin films, (2016).
8. Lundy, R., Byrne, C., Bogan, J., Nolan, K., Collins, M. N., Dalton, E., & Enright, R. (2017). Exploring the role of adsorption and surface state on the hydrophobicity of rare earth oxides. *ACS applied materials & interfaces, 9*, 13751–13760.
9. Fu, S.-P., Rossero, J., Chen, C., Li, D., Takoudis, C. G., & Abiade, J. T. (2017). On the wetting behavior of ceria thin films grown by pulsed laser deposition. *Applied Physics Letters, 110*, 081601.
10. Muñoz-Batista, M. J., Gómez-Cerezo, M. N., Kubacka, A., Tudela, D., & Fernández-García, M. (2014). Role of interface contact in CeO2–TiO2 photocatalytic composite materials. *ACS Catalysis, 4*, 63–72.
11. Wang, X., Jin, Y., & Liang, X. (2017). Significant photocatalytic performance enhancement of TiO2 by CeO2 atomic layer deposition. *Nanotechnology, 28*, 505709.
12. Paušová, Š, Riva, M., Baudys, M., Krýsa, J., Barbieriková, Z., & Brezová, V. (2019). Composite materials based on active carbon/TiO2 for photocatalytic water purification. *Catalysis Today, 328*, 178–182.
13. Waldner, G., & Krysa, J. (2005). Photocurrents and degradation rates on particulate TiO2 layers effect of layer thickness, concentration of oxidizable substance and illumination direction. *Electrochimica Acta, 50*, 4498–4504.
14. Souza, J., Silva, A., & Paes, H. (2007). Synthesis and characterization of CeO 2 thin films deposited by spray pyrolysis. *Journal of Materials Science-materials in Electronics - J MATER SCI-MATER ELECTRON, 18*, 951–956.
15. Konstantinov, K., Stambolova, I., Peshev, P., Darriet, B., & Vassilev, S. (2000). Preparation of ceria films by spray pyrolysis method. *International Journal of Inorganic Materials, 2*, 277–280.
16. Silva, T. G., Ferreira, A., Ribeiro, E., Silveira, E., & Mattoso, N. (2015). Low-defect CeO2 films synthesis by combined spray pyrolysis using different precursors. *Applied Physics A, 118*, 1489–1494.
17. Wang, S., Wang, W., Liu, Q., Zhang, M., & Qian, Y. (2000). Preparation and characterization of cerium (IV) oxide thin films by spray prolysis method. *Solid State Ionics, 133*, 211–215.
18. Elidrissi, B., Addou, M., Regragui, M., Monty, C., Bougrine, A., & Kachouane, A. (2000). Structural and optical properties of CeO2 thin films prepared by spray pyrolysis. *Thin Solid Films, 379*, 23–27.
19. Liu, B., Zhao, X., Zhang, N., Zhao, Q., He, X., & Feng, J. (2005). Photocatalytic mechanism of TiO2–CeO2 films prepared by magnetron sputtering under UV and visible light. *Surface Science, 595*, 203–211.
20. Zlamal, M., Krysa, J., & Jirkovsky, J. (2009). Photocatalytic degradation of acid orange 7 on TiO2 films prepared from various powder catalysts. *Catalysis Letters, 133*, 160–166.
21. Krýsa, J., Paušová, Š, Zlámal, M., & Mills, A. (2012). Photoactivity assessment of TiO2 thin films using acid orange 7 and 4-chlorophenol as model compounds. Part I: key dependencies. *Journal of Photochemistry and Photobiology A: Chemistry, 250*, 66–71.
22. Krysa, J., Waldner, G., Mest'ankova, H., Jirkovsky, J., & Grabner, G. (2006). Photocatalytic degradation of model organic pollutants on an immobilized particulate TiO2 layer - roles of adsorption processes and mechanistic complexity. *Applied Catalysis B-Environmental, 64*, 290–301.
23. Nussbaum, M., Shaham-Waldmann, N., & Paz, Y. (2014). Synergistic photocatalytic effect in Fe Nb-doped BiOCl. *J Photoch Photobio A, 290*, 11–21.
24. Arbell, N., Bauer, K., & Paz, Y. (2021). Kinetic resolution of racemic mixtures via enantioselective photocatalysis. *Acs Applied Materials & Interfaces, 13*, 39781–39790.
25. O. Toker, J. Krysa, Y. Paz, The Effect of Modifying TiO2 with Lanthanides on the Photocatalytic Degradation of Ciprofloxacin, a Hydrophobic Compound, Journal of Photocatalysis, (2022) accepted.
26. Haick, H., & Paz, Y. (2001). Remote photocatalytic activity as probed by measuring the degradation of self-assembled monolayers anchored near microdomains of titanium dioxide. *The Journal of Physical Chemistry B, 105*, 3045–3051.
27. Anderson, C., & Bard, A. J. (1995). An Improved photocatalyst of TiO2/SiO2 prepared by a Sol-Gel synthesis. *The Journal of Physical Chemistry, 99*, 9882–9885.

Authors and Affiliations

Jakub Rusek[1] · Michal Baudys[1] · Omri Toker[2] · Šárka Paušová[1] · Yaron Paz[2] · Josef Krýsa[1]

✉ Josef Krýsa
josef.krysa@vscht.cz

[1] Department of Inorganic Technology, University of Chemistry and Technology Prague, Technická 5, Prague 6 16628, Czech Republic

[2] Department of Chemical Engineering, Technion, 3200003 Haifa, Israel